

MICROSTRIP RESONATORS AND FILTERS USING HIGH-TC SUPERCONDUCTING THIN FILMS ON LaAlO_3

June H. Takemoto, Charles M. Jackson, Roger Hu,
John F. Burch, Kenneth P. Daly, and Randy W. Simon
TRW, Space and Technology Group
One Space Park
Redondo Beach, CA 90278

ABSTRACT

We have measured very low microwave losses in $\text{YBa}_2\text{Cu}_3\text{O}_7$ linear resonators, ring resonators, and bandpass filters. We deposited the 1-2-3 on LaAlO_3 substrates, patterned microwave circuits, and overcoated with a passivating LaAlO_3 layer. HTS linear microstrip resonators demonstrated Q's greater than 1200 at 10 GHz, corresponding to surface resistances less than $300 \mu\Omega$. Identical silver resonators showed Q's of 60 and surface resistance of $15 \text{ m}\Omega$. The high frequency transition temperature for these HTS films was greater than 83 K. We measured Q's of 240 in ring resonators at 15 GHz. Finally, we designed, fabricated, and tested a 2-pole, Chebyshev narrow-bandwidth bandpass filter. The HTS filter was designed to be a 1 percent bandwidth with 0.1 dB ripple. Insertion loss was 2 dB at 4 K, rising to 3 dB at 77 K. We observed temperature dependence in the filter center frequency, which we attribute to kinetic inductance effects. Our HTS filters outperform similar cryogenic silver filters, indicating that practical levels of HTS performance have been achieved.

I. INTRODUCTION

High performance microwave circuits were fabricated with high Tc superconductor (HTS) on LaAlO_3 substrates. Microstrip circuits that use HTS thin films achieve a higher level of microwave performance than circuits using normal metal. The reduction in surface resistance offered by HTS allows a reduction in insertion loss for filter applications. New microstrip resonators can be fabricated with extremely high Q values. Passive microwave components can be integrated into various system applications such as radar, electronic surveillance, and communications.

In this paper, we report measurement results of a variety of HTS resonators and filters designed at different microwave frequencies. From high Q data and microstrip geometry, we can directly analyze the surface resistance and conductor losses of the patterned HTS films. Our patterned microstrip resonators and filters obtained $R_s < 350 \mu\Omega$ after fabrication. These results show that the film degradation was very minimal since unprocessed films have R_s of $50 \mu\Omega$.

Ag microstrip circuits of identical geometries were fabricated and measured for comparison. HTS microwave components were clearly superior to normal metal counterparts. Manufacturing patterned HTS films with quality performance at microwave frequencies is important in demonstrating the immediate applicability of HTS microwave integrated circuit technology. Furthermore, microstrip circuits produced with HTS material achieve a level of microwave performance that cannot be met with normal metal.

II. MICROSTRIP DESIGN

Numerous structures exist for microstrip resonators and filters. Our LaAlO_3 studies include straight 50Ω linear resonators¹, a low impedance resonator with transformer, closed-loop ring resonators², and parallel-coupled, series-gap bandpass filters. Figure 1 shows most of the microstrip circuits reported in this paper. The dielectric constant ϵ_r of LaAlO_3 was determined from these resonator measurements to be 26. LaAlO_3 was chosen as a substrate because the lattice match to YBCO provides high quality films, and its ϵ_r is suitable to microwave applications while the ϵ_r of SrTiO_3 is not.

Manuscript received September 24, 1990.

The 50Ω linear resonators were designed for 10 and 5 GHz. The low impedance resonator was designed for 10 GHz with an impedance transformer from 50 to 25Ω . The coupling gap of the 50Ω linear resonators was varied to investigate the external loading on the resonance and determine the minimum R_s of the HTS films. Resonators with 8, 14, and 20 mil gaps were calculated to have total loaded Q's of about 340, 600, and 1025, respectively.

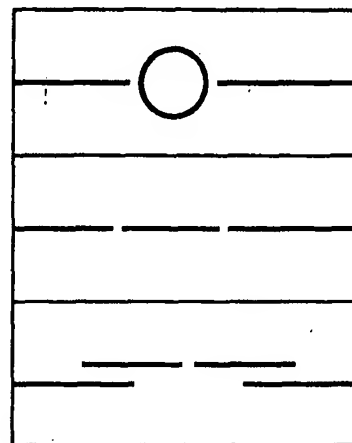


Figure 1. Some of the microstrip circuits tested include (from the top) a 15 GHz- 50Ω ring resonator, a 14-mil gap linear resonator, and a 10 GHz filter.

Ring resonators were designed at 15 GHz with a ring impedance of 40Ω and coupling gap size of 8. The ring diameter for the 40Ω ring was increased to the second harmonic to decrease the ratio of the width to the circumference of the ring. Larger rings minimize field interactions across the ring width and distortion of the field around the coupling gap.³ The drawback of the larger rings is the increased possibility of distorting the uniformity of the ring during fabrication, leading to resonance splitting. The size of the rings was limited to an area of 0.2 in. x 0.5 in. because of the test fixture design. A 10 GHz, 50Ω ring resonator with a 14 mil gap was also tested. These designs were optimized from the previously reported ring resonator design.²

We tested our superconducting microstrip in a practical circuit design using a 2-pole, 0.1 dB ripple, 1 percent bandwidth Chebyshev filter.⁴ Commercial software (TOUCHSTONE) optimized the design. The ϵ_r of 26 for LaAlO_3 is outside the range of ϵ_r that this model can accurately simulate the response of the microstrip designs. Therefore, some feedback from experimental measurements of actual filters was needed to optimize the design. The variety of bandpass filter configurations typically involve either end-coupled or parallel-coupled structures. Since microstrip gaps are not as well modelled as coupled lines, a compromise was made in the filter design (Figure 1). The filter design is parallel coupled in the outer sections and end coupled in the inner sections.

We calculated the effects of kinetic inductance on the design of the resonators and filters. The kinetic energy of the superconducting electron pairs generates inductance, which slows the propagation velocity in the microwave circuit. The larger penetration depth of HTS compared to LTS and the high ϵ_r of LaAlO_3 increases the kinetic inductance effect, producing larger

frequency shifts. At $T/T_c = 0.5$, the kinetic inductance of Nb exhibits a change of 0.7 MHz, while the HTS produces a change of 9.4 MHz. Frequency shifts in the response can also be caused by the change in dielectric constant of the substrate material due to thermal contraction. However, the estimated frequency shift due to this effect is only 0.15 MHz for a 10 K change in temperature. Deviations in the substrate thickness from the nominal 20 mil value contribute significantly to frequency shifts. A $1\mu\text{m}$ change in the microstrip linewidth, which is proportional to the substrate thickness, causes a 2.3 MHz shift in frequency. Therefore, substrates with the same thickness should be selected to accurately incorporate kinetic inductance effects into the design of HTS filters and resonators.

III. PROCESSING

HTS films were sputtered onto whole 1.5-inch diameter LaAlO_3 wafers using a single target of YBCO with a stoichiometric 1-2-3 compound. The substrate was thermally contacted to the platform via silver paste and heated to 700 - 750 °C in an atmosphere of 30 - 50 mT of oxygen and 40 - 200 mT of argon. Off-axis sputtering minimized damage caused by negative ion bombardment. RF power of 125 W provided a film growth of 700 Å/hr. Immediately after deposition, the samples were cooled in 600 T of pure oxygen. The high pressure of oxygen eliminates the need for additional thermal annealing; thus, smooth films suitable for device fabrication can be deposited on substrates.

The baked silver paste was removed and Ag was deposited on the backside of LaAlO_3 to provide a ground plane for the microstrip structures. The HTS was patterned with standard photolithographic techniques and etched with dilute phosphoric acid. Ag or Au contacts were deposited on some of the circuits to improve contacts between K-connector pins and microstrip lines.

Passivation is an important step in practical HTS films to protect them from possible harmful chemicals in its environment. The microwave performance of samples successfully passivated with a LaAlO_3 layer on top of the HTS showed no significant degradation in film quality as evidenced by the high Q-values that were measured. Completed wafers were diced into 0.2 in. x 0.5 in. pieces by a diamond saw. Film deterioration was significantly reduced by shortening the processing time, minimizing the exposure of the HTS solvents and other chemicals, and avoiding ion milling directly on the surface of HTS.

The resultant films yield dc critical temperature of 86 - 91 K with transition widths of 0.5 K. The critical current of the HTS films is $2 \times 10^7 \text{ A/cm}^2$ at 4.2 K and $1 \times 10^6 \text{ A/cm}^2$ at 77 K. Microwave response was superior to copper below 81 - 85 K, indicating that the films are of high quality.

IV. ANALYSIS AND RESULTS

Microstrip circuits were mounted in gold plated OFHC copper test fixtures with either K-connectors or OSM pin connectors suitable for operation up to 18 GHz. Temperature sensors and resistive heaters were attached to the fixture and mounted on the end of a dewar probe which housed two rigid microwave coax cables. Flexible coax cables connected the probe to a HP8720 network analyzer. Microwave switches connected between the device under test and a through-standard provided transmission calibration at any temperature we chose to record resonance data.

Q-factor data from resonators were taken automatically by the HP8720 from the 3 dB points of the transmission response. A typical plot from the network analyzer of a HTS linear resonator with a 20 mil gap is shown on Figure 2. The samples were first cooled to liquid helium. As they were gradually warmed, their center frequency, Q factor, and insertion loss were recorded as a function of temperature. Plots of these parameters against temperature showed the sharp temperature transition of HTS at microwave frequencies.

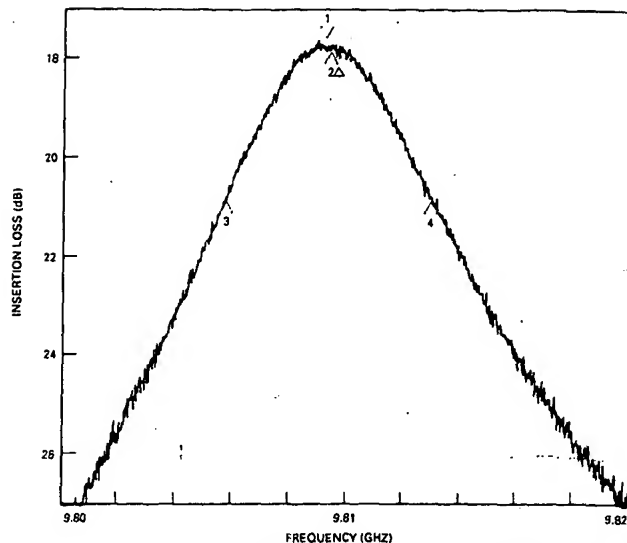


Figure 2. Typical plot of resonance data from HP8720 network analyzer. Markers 1 and 2 show data at minimum insertion loss and center frequency, and markers 3 and 4 point the 3-dB bandwidth. Above is the transmission response of linear resonator with a 20 mil coupling gap.

The resonance frequency versus temperature data clearly showed kinetic inductance effects. Figure 3 shows the plot of resonance frequency of a linear resonator as a function of temperature. The plot shows the rapid shift in resonance frequency near T_c where most of the transformation of normal electrons into superconducting electrons occur. The shift in frequency itself is directly caused by the kinetic inductance of the superconducting electrons.

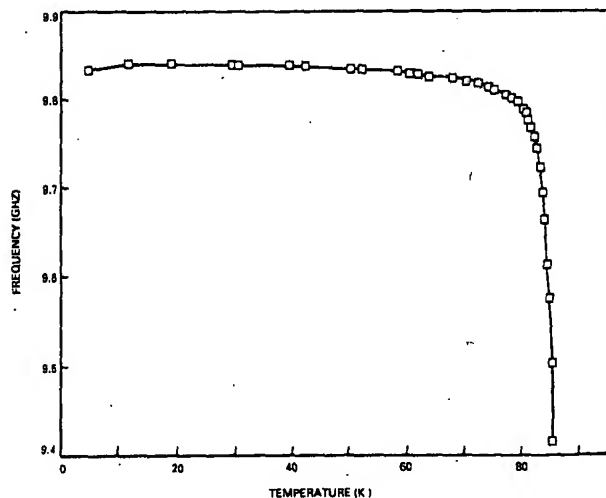


Figure 3. The plot of resonant frequency versus temperature demonstrates kinetic inductance effects in HTS circuits.

Values of surface resistance, R_s , and conductor losses, α_c , were calculated from the measured Q. Consideration must be made for a microstrip in which the material for the top conductor is different from the bottom ground plane since our HTS circuits had Ag ground planes. The extra loss due to the normal metal Ag were determined from Pucel's equations.⁵

$$w' = w + \frac{t}{\pi} \left[\ln \left(\frac{2h}{t} \right) + 1 \right]$$

$$B = 1 - \frac{w'^2}{16h^2}$$

$$C = \frac{1}{h} \left(1 - \frac{t}{\pi w'} \right)$$

$$D = \frac{2}{w'} \left[1 + \frac{1}{\pi} \ln \left(\frac{2h}{t} \right) \right]$$

$$R_s = \frac{4\pi^2 Z_0}{\lambda_g B(2C+D)Q}$$

where
 w = microstrip line width of the resonator
 h = substrate thickness
 t = thickness of the conducting film
 Z_0 = characteristic impedance of the resonator
 Q = unloaded Q of the resonator.
 λ_g = guide wavelength

Since no attempt was made to accurately determine the coupling coefficient of the resonators,⁶ we approximated that the measured Q is closely equal to the unloaded (intrinsic) Q of the circuit. This is true only for loosely coupled resonators, i. e. samples with large gap sizes, since $1/Q_L = 1/Q_0 + 1/Q_{ext}$, where Q_L is the total loaded Q , Q_0 is the unloaded Q , and Q_{ext} is the external Q . When the extra loss due to the normal metal ground plane was included into the calculations, the HTS film surface resistance, R_{ss} , was determined using the following equation:

$$R_{ss} = R_{sa} - \frac{4\pi^2 Z_0}{\lambda_g B(C+D)} \left(\frac{1}{Q_a} - \frac{1}{Q_s} \right)$$

where,
 Q_a = measured Q from Ag resonator
 Q_s = measured Q from HTS resonator with Ag ground plane
 R_{sa} = surface resistance of normal metal ground plane determined from Q_a .

α_c of HTS and Ag can be determined independently from R_{ss} and R_{sa} from the relationship, $\alpha_c = \pi / \lambda_g Q$.

The surface resistances of our patterned HTS films (about 40 in total) all measured less than 500 $\mu\Omega$. This value of R_s is more than 10 times better than the R_s of Cu. R_s of unpatterned films was typically 50 $\mu\Omega$ when measured using the method developed by Taber.⁷ In other words, the HTS films degraded no more than 10 times after patterning. The best R_s obtained from an HTS circuit was less than 350 $\mu\Omega$, only 7 times worse than the fresh films.

Low impedance resonators at Q 's of about 200 at 10 GHz, which is generally worse than linear resonators due to higher coupling. Ring resonators at 15 GHz attained a Q of 230. The highest Q obtained for HTS linear resonators designed at 10 GHz with coupling gaps of 8, 14, and 20 mils were 600, 1200, and 1400, respectively. These Q 's were higher than the expected values (refer to section II) calculated from microwave simulations. A Ag linear resonator of dimensions identical to the 8 mil sample yielded a Q of 63. The external loading was estimated to be sufficiently small even at a gap of 8 mils.

The HTS resonator of all three gap sizes and the Ag resonator were measured as a function of increasing temperature. Figure 4 which displays Q versus temperature of all of these circuits, graphically depicts the higher microwave performance of the HTS films over their Ag counterparts. The highest HTS Q of 1400 is more than 20 times better than Ag. Following the analysis outlined in section IV, both the surface resistance and conductor attenuation of HTS and Ag films were calculated.

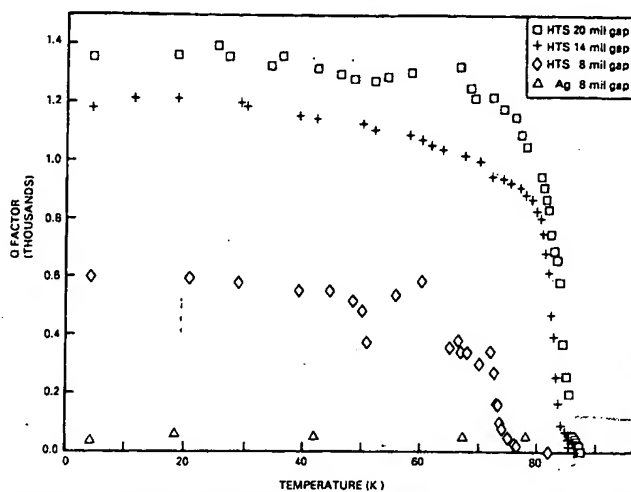


Figure 4. Q versus temperature of the three HTS linear resonators with 8, 14, and 20 mil coupling gaps and the Ag linear resonator with an 8 mil gap.

The performance of the 8 mil Ag linear resonator was compared to the 14 mil HTS linear resonator to assess an HTS Q value that is not limited to the external Q of the resonator design. The equations in the previous section with $Q_a = 63$ and $Q_s = 1200$ lead to surface resistance values of $R_{sa} = 18 \text{ m}\Omega$ and $R_{ss} = 350 \mu\Omega$. Refer to section IV for the definition of the variables. Since Q_s is larger for larger gap resonators, we can safely conclude that $R_{ss} < 350 \mu\Omega$. The conductor attenuation constant of both Ag and HTS can be calculated from R_{sa} and R_{ss} as $\alpha_{ca} = 1.6 \times 10^{-3} \text{ dB/mm}$ and $\alpha_{css} = 3.2 \times 10^{-5} \text{ dB/mm}$, respectively.

Finally, the HTS 2-pole filters showed lower insertion losses than equivalent Ag filters. Two filters each designed for the same performance were fabricated; one using HTS, and the other using Ag. Filters were evaluated by observing their frequency selectivity and insertion loss. Figure 5 clearly demonstrates better rejection and out of band response of the HTS filter compared to the Ag filter.

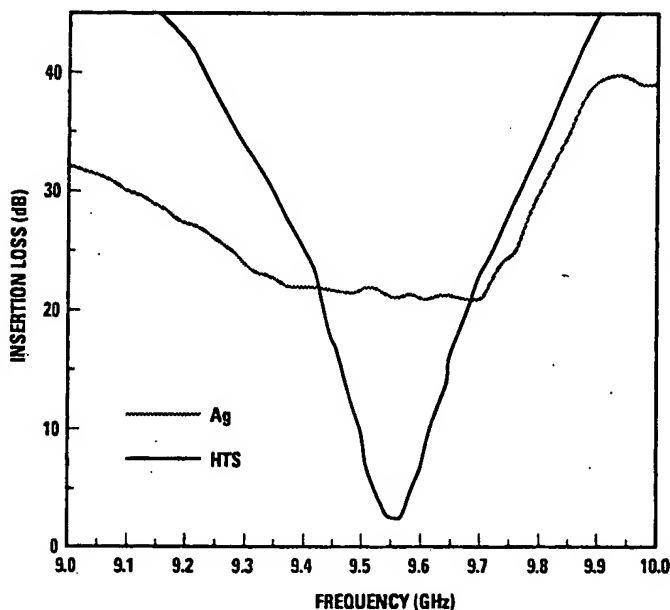


Figure 5. 10 GHz filter response of HTS and Ag on LaAlO_3 . HTS filter shows a much higher frequency selectivity and lower insertion loss than the Ag filter.

Th HTS filter response changes very little from liquid helium temperatures up to 60K. The insertion loss of HTS filters was about 2 dB compared to the insertion loss of Ag filters, which was greater than 20 dB. HTS filter insertion losses began increasing at about 77 K. The bandwidth of the HTS filters was about 50 MHz, while the Ag filters had bandwidths of about 400 MHz. The HTS filters closely matched the designed filter bandwidth.

VI. CONCLUSIONS

We have successfully used HTS films to fabricate microstrip resonators and filters that respond at several microwave frequencies. These microwave circuits yield high microwave performances that were superior to the same circuits using normal metals. The most practical circuit we designed was a 2-pole Chebyshev filter. The HTS filter had a 2 dB insertion loss which was much lower than that of the Ag filter. Our improved processing technique, which includes LaAlO_3 passivation, inflicts little damage to our high quality 1-2-3 films on LaAlO_3 . We achieved surface resistances of less than $350 \mu\Omega$ at 10 GHz for our patterned films of HTS. The higher level of performance of HTS microstrip circuits allows us to apply high-Tc superconductivity to integrated circuit technology.

ACKNOWLEDGEMENTS

This research was funded by SDIO under contract number: SDIO84-88-C-0047.

REFERENCES

1. E. Belohoubek and E. Denlinger, "Loss Considerations for Microstrip Resonators," *IEEE Trans. Microwave Theory and Tech.*, vol. MTT-23, pp. 522-526, 1975
2. J. H. Takemoto, F. K. Oshita, H. R. Fetterman, P. Kobrin, E. Sovero, "Microstrip Ring Resonator Technique for Measuring Microwave Attenuation in High Tc Superconducting Thin Films," *IEEE Trans. Microwave Theory and Tech.*, vol. MTT-37, pp. 1650-1652, Oct. 1989.
3. T. C. Edwards, Foundations for Microstrip Circuit Design, John Wiley and Sons, N.Y., 1981.
4. G. L. Matthaei, L. Young, and E.M.T. Jones, Microwave Filters, Impedance-Matching Networks, and Coupling Structures, Aertech House, Dedham MA, 1964.
5. R. A. Pucel, D. S. Masse, and C. P. Hartwig, "Losses in Microstrip," *IEEE Trans. Microwave Theory and Tech.*, vol. MTT-16, pp. 342-350, June 1968; Correction, vol. MTT-16 pp. 1064, Dec. 1968.
6. J. Aitken, "Swept-frequency microwave Q-factor measurements," *Proc. Inst. Elec. Eng.*, vol. 123, no. 9, pp. 855-862, Sept. 1976.
7. R. C. Taber, et. al., "Microstructure and RF Properties of $\text{YBa}_2\text{Cu}_3\text{O}_7$ Thin Films," *Bulletin of the APS*, Vol. 35, No. 3, session S14-7, pp. 811, APS March Meeting 1990.

m
Y
3-
pa
13
6
thi
us
qu
fil
cr
fal
9:
Yl
the

fil
(Y
ste
su
the
po
ori
pri
be
an
to
fil
we
as
cal
an
de
po
de
tec
no
co

Th

sin
sid
iso
cle
dei
epi
pei
du
car
rot
obi
tin
pre
rat
of